

Kaul et al _Inventory of Supplemental Materials

Supplemental Figures and Figure Legends

Figure S1, related to Figure 1

Figure S2, related to Figure 2

Figure S3, related to Figure 3

Figure S4, related to Figure 4

Supplemental Materials and Methods

Supplemental Tables

Supplemental Table 1. Plasmids.

Supplemental Table 2. Antibodies.

Supplemental References

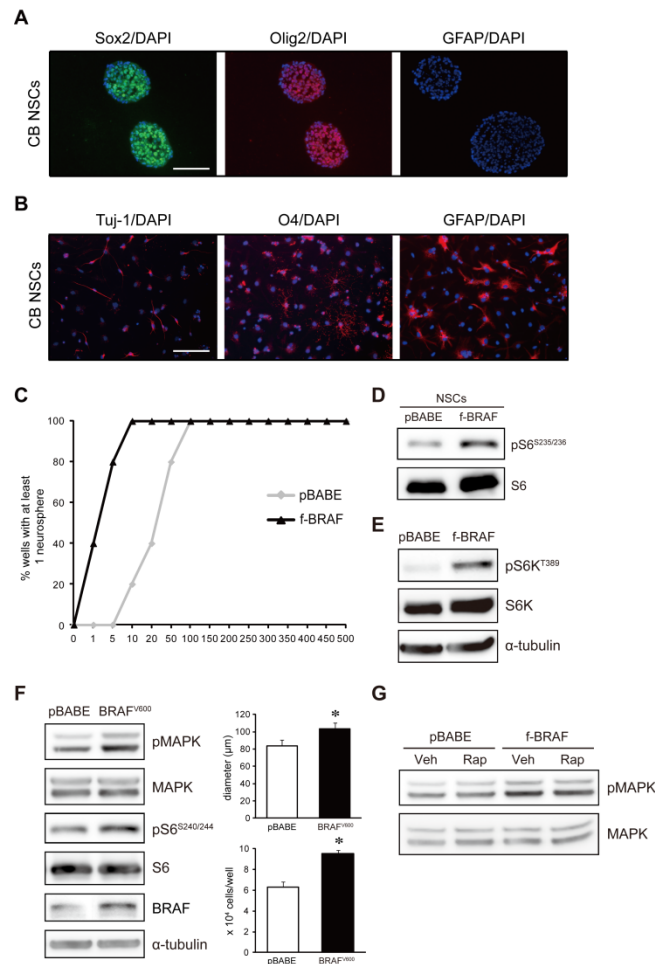


Figure S1. f-BRAF and BRAF^{V600} activate mammalian target of rapamycin (mTOR) in cerebellar NSCs. (A) Neurospheres generated from the cerebellum are positive for Sox2 (green) and Olig2 (red) expression, but negative for GFAP expression, and (B) can give rise to neurons (Tuj-1⁺), oligodendrocytes (O4⁺) and astrocytes (GFAP⁺). Nuclei are counterstained with DAPI. (C) Following f-BRAF expression, fewer NSCs are required to generate individual neurospheres (limiting dilution assay), and there is increased (D) S6 and (E) S6-Kinase (S6K) phosphorylation. (F) BRAF^{V600} expression in cerebellar NSCs results in increased MAPK and mTOR (phospho-S6) activation, as well as increased NSC proliferation. (G) Rapamycin treatment does not reduce f-BRAF-induced MAPK activation. pBABE, control virus; Veh, vehicle; Rap, rapamycin. Error bars denote mean \pm SD. (*) $p < 0.01$. Scale bars: 100 μ m.

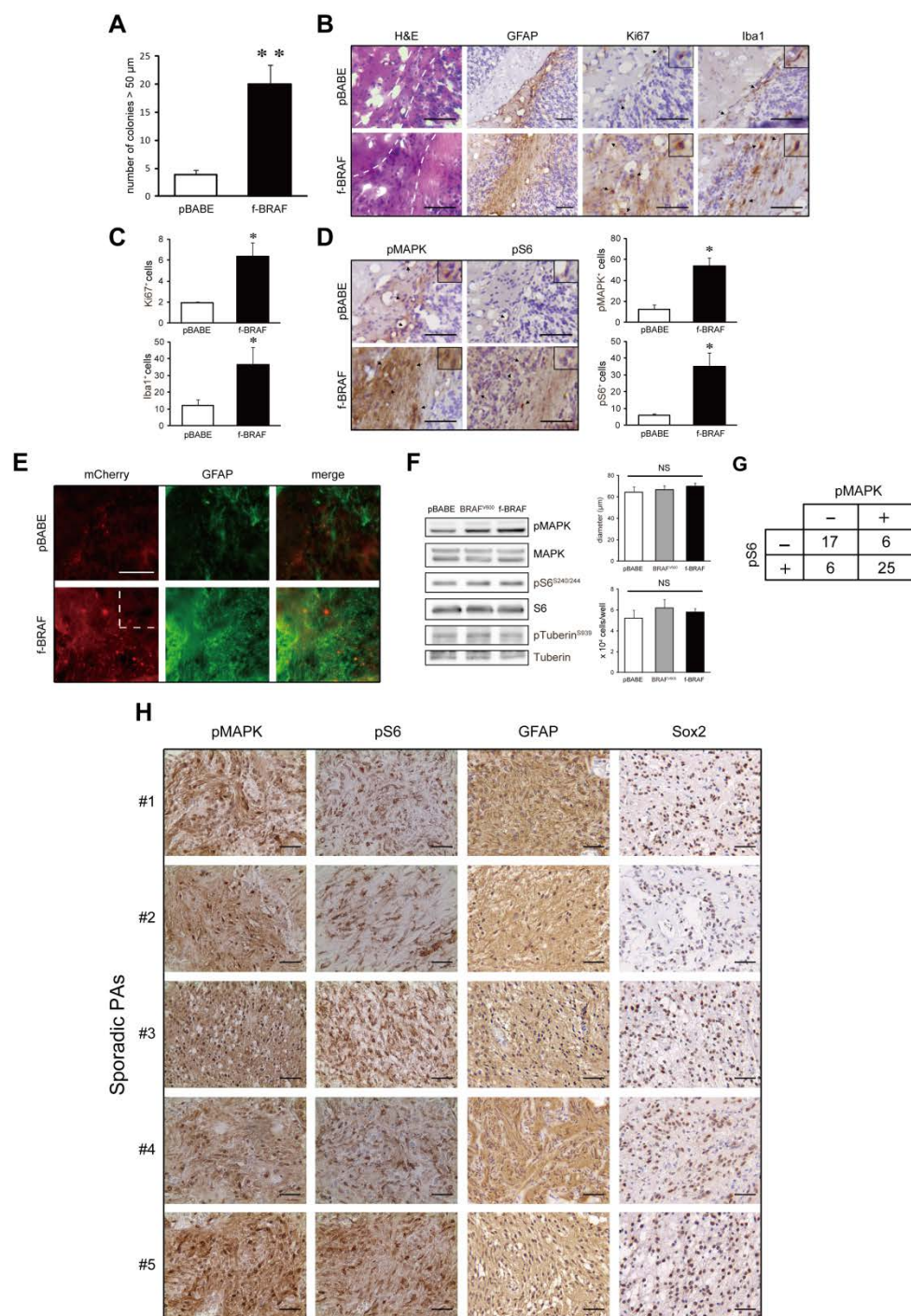


Figure S2. mTOR activation in human sporadic PAs. (A) Compared to pBABE-infected (control) NSCs, f-BRAF-expressing NSCs form 5-fold more colonies in soft agar. (B) Representative images of the injection site (dotted lines) at 2.5 months post-enugraftment with mCherry⁺ pBABE- or f-BRAF-expressing NSCs reveal mild increase in cellularity (H&E) and GFAP immunoreactive

cells. There are 3-fold increases in the numbers of Ki67⁺ (arrows and inset; *C*) and Iba1⁺ cells (arrows and inset; *C*) in the areas around the BRAF-expressing NSC injection sites. (*D*) Increased pMAPK (arrows and inset; quantification, right) and pS6 (arrows and inset; quantification, right) immunoreactivity are observed in the areas around the BRAF-expressing NSC injection sites. (*E*) Immunofluorescence co-labeling of mCherry and GFAP shows distinct GFAP⁺ cell populations in the areas around the f-BRAF-expressing NSC injection sites, either co-labeling with both markers (yellow) or labeling with GFAP only (area within the dotted box). (*F*) Neither f-BRAF nor BRAF^{V600} expression increase the proliferation of cortical NSCs. While both f-BRAF and BRAF^{V600} expression increased MAPK phosphorylation, there are no changes in tuberin or S6 phosphorylation. (*G*) pS6 and pMAPK are coordinately expressed in human sporadic PAs ($p < 0.0001$, Chi-squared test). (*H*) Five representative f-BRAF-containing PA cases exhibit increased MAPK phosphorylation, mTOR activation (S6 phosphorylation) and GFAP and Sox-2 immunoreactivity. Error bars denote mean \pm SD. (**) $p < 0.005$, (*) $p < 0.05$. Scale bars: 50 μ m. NS, not significant.

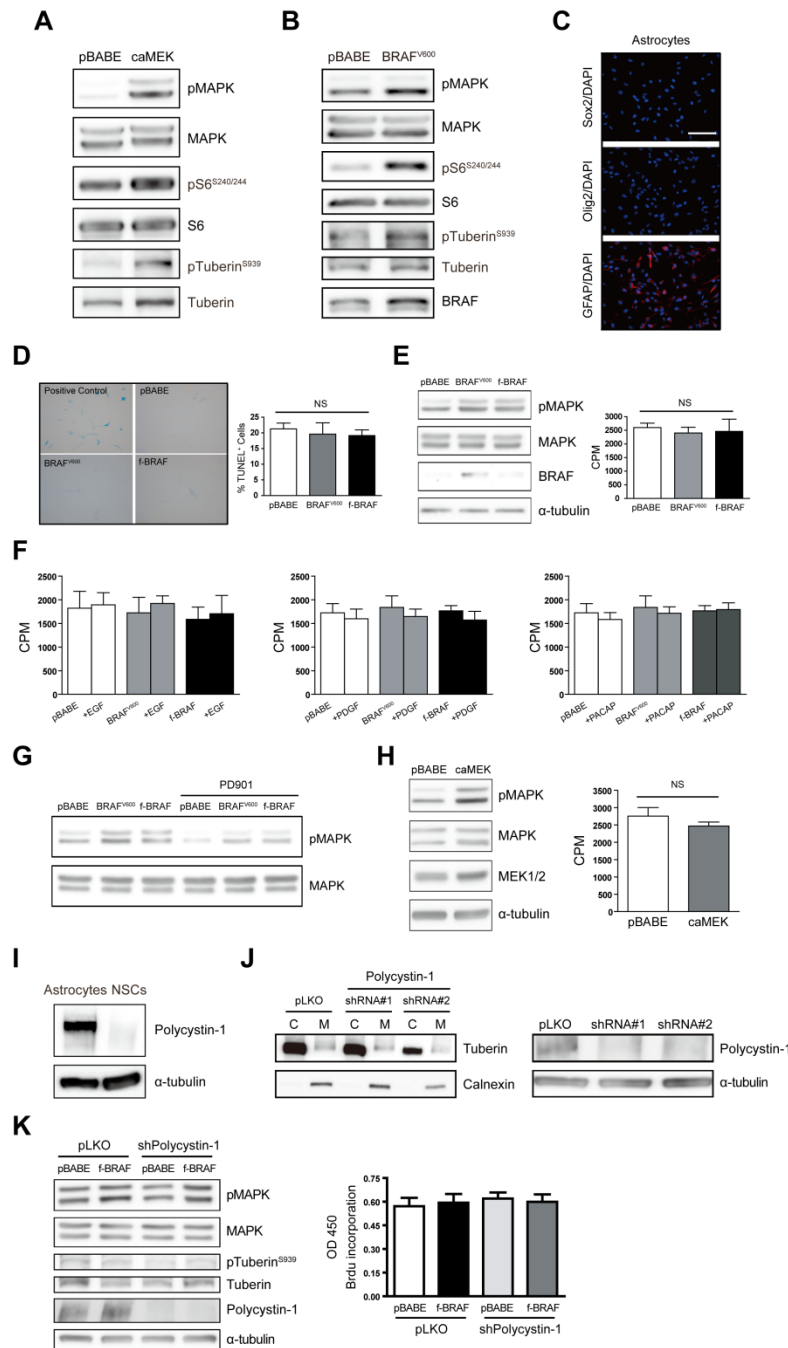


Figure S3. f-BRAF expression does not increase astrocyte proliferation. (A) Constitutively-activate MEK (caMEK) and (B) BRAF^{V600} expression in cerebellar NSCs results in increased tuberin phosphorylation. (C) Cerebellar astrocytes are GFAP⁺, but Sox- and Olig2-negative. Nuclei are counterstained with DAPI. (D) No increase in cellular senescence (β-galactosidase (β-gal) cytochemistry; left) or apoptosis (TUNEL labeling; right) is observed following BRAF^{V600}

or f-BRAF expression in cerebellar astrocytes. Endogenous acidic β -gal activity serves as a positive control. (E) Both BRAF^{V600} and f-BRAF expression in forebrain astrocytes induce increased MAPK activation (phosphorylation), but no change in proliferation (thymidine incorporation; CPM). α -tubulin serves as an internal loading control. (F) Astrocyte proliferation following BRAF^{V600} and f-BRAF expression is not increased in response to epidermal growth factor (EGF), platelet-derived growth factor (PDGF), or pituitary adenylate cyclase-activating peptide (PACAP) exposure. (G) Increased MAPK phosphorylation induced by BRAF^{V600} and f-BRAF is reduced following treatment with the MEK inhibitor PD0325901 (PD901; 10nM). (H) caMEK expression in cerebellar astrocytes increases MAPK activation, with no change in proliferation. (I) Increased polycystin-1 expression is observed in astrocytes relative to NSCs. α -tubulin is included as an internal protein loading control. (J) Polycystin-1 knockdown in wild-type astrocytes, using two different shRNA constructs, results in a 75% and 78% reduction in polycystin-1 expression, respectively (right), but does not change tuberin subcellular localization (left). (K) Polycystin-1 KD does not increase proliferation (ELISA-based BrdU incorporation) or tuberin phosphorylation in f-BRAF-expressing astrocytes. Error bars denote mean \pm SD. NS, not significant. Scale bar: 100 μ m.

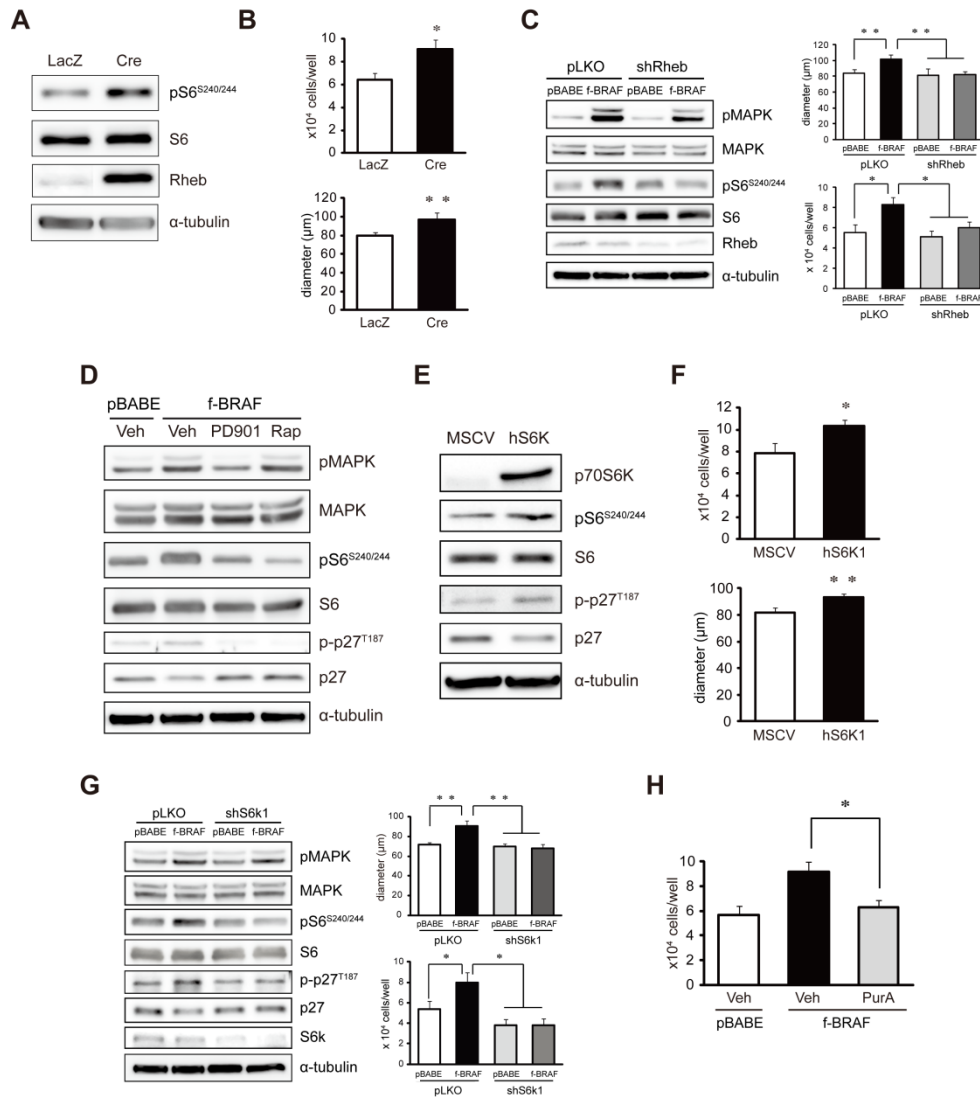


Figure S4. f-BRAF regulation of NSC proliferation requires Rheb-mediated mTOR/S6K activation and p27 degradation. (A) Rheb overexpression in cerebellar NSCs, following Ad5Cre (Cre) infection, results in increased S6 phosphorylation. Ad5LacZ (LacZ) infection generates wild-type control cells. (B) Rheb overexpression induces increased cerebellar NSC proliferation, as assessed by both direct cell counting and secondary neurosphere diameters. (C) Rheb knockdown using a second shRNA construct similarly inhibits S6 phosphorylation and f-BRAF-induced cerebellar NSC proliferation, as assessed by both secondary neurosphere diameters and direct cell counting. (D) f-BRAF expression in cerebellar NSCs results in increased p27 phosphorylation and decreased p27 expression, which is attenuated following PD901 (2 nM)

and rapamycin (0.2 nM Rap) treatment. (E) hS6K1 overexpression in cerebellar NSCs results in increased mTOR activation (S6 phosphorylation), increased p27 phosphorylation, and decreased p27 levels. (F) hS6K1 overexpression increases cerebellar NSC proliferation as assessed by direct cell counting and secondary neurosphere diameters. MSCV-GFP was used as control. (G) S6k1 knockdown using a second shRNA construct similarly inhibits f-BRAF-induced S6 and p27 phosphorylation, and restores p27 to wild-type levels. α -tubulin was included as an internal protein loading control. (H) Treatment of f-BRAF-expressing cerebellar NSCs with the cdk2 inhibitor (PurA) reduces proliferation (cell number) to wild-type levels. Veh, vehicle. Error bars denote mean \pm SD. (*) $p < 0.01$, (**) $p < 0.05$.

Supplemental Materials and Methods

Adenovirus and retroviral infections. Ad5-LacZ and Ad5-Cre (University of Iowa Gene Transfer Core, Iowa City, IA) infection was used to generate wild-type and Rheb-overexpressing NSCs, respectively. Control and hS6K1-overexpressing NSCs were generated following infection with MSCV-GFP or MSCV-hS6K1 retrovirus, respectively, as previously described (Uhlmann et al., 2004).

Multi-lineage differentiation and limiting dilution assay. NSC differentiation and limiting dilution analyses were performed as previously described (Dasgupta and Gutmann, 2005; Lee et al., 2010)

Soft agar colony forming assay. Neural stem cell media was mixed with melted agarose in water (0.6% agar), which was layered into 6 well plates to form the bottom agar. Neurospheres were trypsinized, mixed with soft agarose/neural stem cells media mixture (0.3%) and plated at 20,000 cells per well. The top agar, containing the NSCs was allowed to polymerize and 2 mls of normal NSC growth media was then layered on top of the polymerized agar. Cultures were incubated for 4 weeks and viable colonies visualized by incubating with 5% MTT in PBS for 1hr at 37°C.

Analysis of TMA tumors. Sporadic PAs were analyzed using a previously-generated tissue microarray (TMA;(Tibbetts et al., 2009). Tumors were scored as “negative” when <25% cells were immunopositive and “positive” when >50% of the tumor cells were immunopositive. Scored tumor samples were analyzed using the chi-square test of association.

Senescence assay and TUNEL labeling. The senescence-associated β -galactosidase (SA- β gal) assay was performed as previously reported (Debacq-Chainiaux et al., 2009) following fixation in 4% paraformaldehyde. Terminal deoxynucleotidyl transferase-mediated dUTP nick end labeling (TUNEL) labeling was performed using a fluorescence-based in situ cell death detection kit (Roche Diagnostics).

Cell proliferation using BrdU ELISA. Astrocyte proliferation (8000 cells/well in a 96-well plate) was assessed using the BrdU Cell Proliferation ELISA kit (Roche), following the manufacturer's instructions. Briefly, cells were labeled with BrdU for 16 hrs in serum free medium, and proliferating cells identified using a peroxidase-conjugated Anti-BrdU antibody by colorimetric substrate reaction measured at 450nm using a spectrophotometer.

Supplemental Table 1. Plasmids.

<u>Construct</u>	<u>Source</u>
<i>KIAA1549-BRAF(16-9)pBABEpuro</i>	Dr. Peter Collins, University of Cambridge
<i>MEKQ56PpBABEpuro</i>	Dr. Jason Weber, Washington University
<i>BRAFV600EpBABEpuro</i>	Dr. Graeme Hodgson, University of California, San Francisco
<i>mCherryFUW</i>	Dr. Josh Rubin, Washington University
<i>shRheb</i> NM_053075.2, TRCN0000075607	Sigma
<i>shRheb</i> NM_053075.2, TRCN0000075605	Sigma
<i>shS6k1</i> NM_028259.1, TRCN0000022905	Sigma
<i>shS6k1</i> NM_028259.1, TRCN0000022904	Sigma
<i>shPolycystin-1</i> NM_013630.2, TRCN00000304612	Sigma
<i>shPolycystin-1</i> NM_013630.2, TRCN000003046664	Sigma
<i>pLKO.1</i>	Sigma
<i>p5R_IRESGFP (MSCV vector)</i>	Dr. Jason Weber, Washington University

Supplemental Table 2. Antibodies.

<u>Antibody</u>	<u>Host</u>	<u>Source</u>	<u>Dilution</u>
BRAF	Rabbit	Abcam	1:500
Calnexin	Rabbit	Enzo	1:5000
GFAP (IHC, ICC)	Rat	Invitrogen	1:200
GFAP (IHC)	Mouse	Millipore	1:500
Hamartin	Mouse	Invitrogen	1:1000
Iba1 (IHC)	Rabbit	Wako	1:1000
Ki67 (IHC)	Mouse	BD Pharmingen	1:500
MAPK	Rabbit	Cell Signaling	1:2000
MEK1/2	Rabbit	Cell Signaling	1:1000
O4(ICC)	Mouse	Chemicon	1:1000
Olig2(ICC)	Rabbit	Gift from Prof. Charles Stiles, Dana Farber Cancer Institute, Boston, MA	1:10,000
p27	Rabbit	Cell Signaling	1:2000
p70S6-kinase	Rabbit	Cell Signaling	1:1000
phospho-MAPK ^{Thr202/Tyr204} (WB and IHC)	Rabbit	Cell Signaling	1:5000
phospho-p27 ^{Thr187}	Rabbit	Abcam	1:500
phospho-p70S6-kinase	Rabbit	Cell Signaling	1:1000
phospho-RSK ^{Thr573}	Rabbit	Cell Signaling	1:1000
phospho-S6 ^{Ser235/236}	Rabbit	Cell Signaling	1:1000
phospho-S6 ^{Ser240/244} (WB and IHC)	Rabbit	Cell Signaling	1:5000
phospho-Tuberin ^{Ser939}	Rabbit	Cell Signaling	1:1000
Polycystin-1	Mouse	Abcam	1:500
Rheb	Rabbit	Cell Signaling	1:500
RSK (p90-RSK)	Rabbit	Cell Signaling	1:1000
S6	Rabbit	Cell Signaling	1:2000
Sox2(ICC)	Mouse	Abcam	1:10,000
Sox2(IHC)	Mouse	Cell Signaling	1:20
Tuberin	Rabbit	Cell Signaling	1:1000
Tuj-1(ICC)	Mouse	Covance	1:1000
α -tubulin	Mouse	Sigma	1:20,000

WB: Western Blot, IHC: Immunohistochemistry, ICC: Immunocytochemistry

Supplemental References

Dasgupta, B., and Gutmann, D. H. (2005). Neurofibromin regulates neural stem cell proliferation, survival, and astroglial differentiation in vitro and in vivo. *J Neurosci* 25, 5584-5594.

Debacq-Chainiaux, F., Erusalimsky, J. D., Campisi, J., and Toussaint, O. (2009). Protocols to detect senescence-associated beta-galactosidase (SA-beta-gal) activity, a biomarker of senescent cells in culture and in vivo. *Nat Protoc* 4, 1798-1806.

Lee, D. Y., Yeh, T. H., Emnett, R. J., White, C. R., and Gutmann, D. H. (2010). Neurofibromatosis-1 regulates neuroglial progenitor proliferation and glial differentiation in a brain region-specific manner. *Genes Dev* 24, 2317-2329.

Tibbetts, K. M., Emnett, R. J., Gao, F., Perry, A., Gutmann, D. H., and Leonard, J. R. (2009). Histopathologic predictors of pilocytic astrocytoma event-free survival. *Acta Neuropathol* 117, 657-665.

Uhlmann, E. J., Li, W., Scheidenhelm, D. K., Gau, C. L., Tamanoi, F., and Gutmann, D. H. (2004). Loss of tuberous sclerosis complex 1 (Tsc1) expression results in increased Rheb/S6K pathway signaling important for astrocyte cell size regulation. *Glia* 47, 180-188.